

OAK RIDGE NATIONAL LABORATORY LIBRARIES



3 4456 0548322 3

ORNL-3677
UC-25 -- Metals, Ceramics, and Materials
TID-4500 (34th ed.)

EVAPORATION OF IRON-, NICKEL-, AND
COBALT-BASE ALLOYS AT 760 TO 980°C
IN HIGH VACUUMS

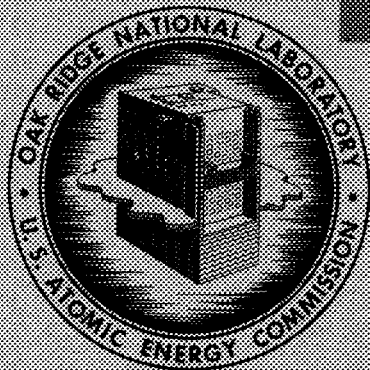
D. T. Bourgette

OAK RIDGE NATIONAL LABORATORY
CENTRAL RESEARCH LIBRARY
CIRCULATION SECTION
4500N ROOM 175

LIBRARY LOAN COPY

DO NOT TRANSFER TO ANOTHER PERSON.
If you wish someone else to see this report, send in
name with report and the library will arrange a loan.

ORNL 118 (6-67)



OAK RIDGE NATIONAL LABORATORY

operated by

UNION CARBIDE CORPORATION

for the

U. S. ATOMIC ENERGY COMMISSION

LEGAL NOTICE

This report was prepared as an account of Government sponsored work. Neither the United States, nor the Commission, nor any person acting on behalf of the Commission:

- A. Makes any warranty or representation, expressed or implied, with respect to the accuracy, completeness, or usefulness of the information contained in this report, or that the use of any information, apparatus, method, or process disclosed in this report may not infringe privately owned rights; or
- B. Assumes any liabilities with respect to the use of, or for damages resulting from the use of any information, apparatus, method, or process disclosed in this report.

As used in the above, "person acting on behalf of the Commission" includes any employee or contractor of the Commission, or employee of such contractor, to the extent that such employee or contractor of the Commission, or employee of such contractor prepares, disseminates, or provides access to, any information pursuant to his employment or contract with the Commission, or his employment with such contractor.

ORNL-3677

Contract No. W-7405-eng-26

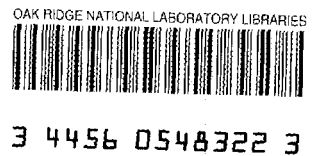
METALS AND CERAMICS DIVISION

EVAPORATION OF IRON-, NICKEL-, AND COBALT-BASE ALLOYS
AT 760 TO 980°C IN HIGH VACUUMS

D. T. Bourgette

NOVEMBER 1964

OAK RIDGE NATIONAL LABORATORY
Oak Ridge, Tennessee
operated by
UNION CARBIDE CORPORATION
for the
U.S. ATOMIC ENERGY COMMISSION



U

8

EVAPORATION OF IRON-, NICKEL-, AND COBALT-BASE ALLOYS
AT 760 TO 980°C IN HIGH VACUUMS

D. T. Bourgette

ABSTRACT

Evaporation rates of types 316, 304, and 446 stainless steels, Inconel, INOR-8, and Haynes alloy No. 25 were measured at pressures ranging from 5×10^{-7} to 1×10^{-9} torr in both the polished and oxidized conditions to determine their suitability for use in high vacuums.

Evaporation losses increased with chromium and manganese concentration and temperature but were independent of pressure in the range investigated. The data have also shown that, at constant temperature, the evaporation rates decreased with time and that the lower the test temperature the greater was the decrease in the rate.

Metallographically, the manifestations of evaporation were subsurface void formation, grain growth at the specimen surface, excessive void formation in the grain boundaries, disappearance of precipitated phases, and materials loss from the edges of surface grains. Chemically, chromium and manganese were found to be the principal elements lost; however, lesser amounts of Fe, Ni, Co, C, and Si were found in the vapor deposits. Microprobe analysis revealed the existence of chromium and manganese concentration gradients that changed with time.

At test temperatures of 872 and 982°C, it was found that a thin film of Cr_2O_3 (the most stable oxide studied) retarded the evaporation of the base alloy; however, the protection was not permanent. After approximately 1000 to 3000 hr, the evaporation rates for both the oxidized and polished surfaces of type 316 stainless steel were nearly equal.

In the case of type 316 stainless steel, the alloy most thoroughly studied, the evaporation rates for the polished condition varied from 5.23×10^{-5} mg/cm²/hr at 760°C to 6.60×10^{-3} mg/cm²/hr at 982°C. While, for the oxidized condition (Cr_2O_3 film), the evaporation rates varied from 4.44×10^{-4} mg/cm²/hr at 872°C to 3.57×10^{-3} mg/cm²/hr at 982°C, at 760°C an oxidized specimen suffered no weight loss in 1142 hr.

It was concluded that multicomponent alloys, unlike pure metals, evaporated nonlinearly with time and that this evaporation resulted in preferential loss of the higher vapor pressure elements. Further, these changes in composition may result in important changes in the physical and mechanical properties of the alloy.

INTRODUCTION

This report summarizes the evaporation behavior of Inconel, INOR-8, Haynes alloy No. 25, and types 304, 316, and 446 stainless steels between 760 and 982°C in vacuums of 5×10^{-7} to 1×10^{-9} torr for times up to 3500 hr with major emphasis directed toward the study of type 316 stainless steel. The investigation encompasses measurements of the evaporation rates, identification of the evaporating elements, and correlation of these measurements to the alloy composition for specimens in both the polished and oxidized conditions.

Although the practicality of using the above alloys up to 982°C has been demonstrated for a variety of environments, the concept of their use in the hard vacuum of space, as indicated in Table 1, is unique and has not been shown to be feasible.¹

A potential and perhaps serious problem arises regarding the stability of the alloys, because pure metals and multicomponent alloys vaporize when heated to elevated temperatures in vacuum. The evaporation rate of a pure element or a simple compound evaporating as a monomolecular vapor is related to its vapor pressure p and molecular weight M by the Knudsen-Langmuir equation

$$W = \alpha p / (2\pi RT/M)^{1/2}$$

where W is the evaporation rate, α is the evaporation coefficient, generally equal to 1, and the other symbols have their conventional meaning.

The usefulness of this expression in estimating the vaporization rates of multicomponent alloys is doubtful since a large source of error arises not so much from an estimation of the molecular weight of the alloy vapor as from a determination of the vapor pressure. Because selective evaporation losses of the more volatile elements are a distinct possibility, the surface composition could become progressively enriched with lower vapor pressure elements and bear no resemblance to the original surface. The theoretical losses based on the Knudsen-Langmuir

¹F. S. Johnson, Satellite Environment Handbook, Stanford University Press, Stanford, Calif., 1961.

Table 1. Characteristics of Space Environments
at Various Altitudes

Altitude (miles)	Molecular Weight	Particles (No./cm ³)	Density (g/cm ³)	Pressure (torr)	Constituents and Proportions
0	29	2.5×10^{19}	1.22×10^{-3}	760	21% O ₂ -79% N ₂
300 ^a	16.6	1.44×10^8	4.10×10^{-15}	2.17×10^{-8}	88% O-5% N-7% N ₂
300 ^b	15.9	1.20×10^7	3.10×10^{-16}	1.24×10^{-9}	91% O-8% N-1% N ₂
1000 ^a	8.3	1.00×10^4	1.35×10^{-19}	5.10×10^{-12}	46% O-8% N-46% H
1000 ^b	1.0	3.7×10^4	6.3×10^{-20}	3.87×10^{-12}	100% H
Interplane- tary space ^c	1.0	30	5.02×10^{-24}	5×10^{-16}	100% H

^aAt maximum sunspot activity.

^bAt minimum sunspot activity.

^cValues from NRC literature.

equation are expected to be representative only of the initial alloy and would give high estimates when applied to the tests in this investigation.

The purpose of this investigation, therefore, was to determine the high vacuum stability of certain iron-, nickel-, and cobalt-base alloys with regard to their compositional, surface, and microstructural behavior. It was felt that this approach would: (1) provide a value for the initial evaporation rate, (2) indicate changes in this initial rate caused by a dynamically changing composition, surface structure, and microstructure, and (3) suggest methods by which evaporation losses might be minimized.

EXPERIMENTAL

Sample Preparation

As-received specimen stock 0.16 to 0.48 cm in thickness was further cold rolled to thicknesses ranging from 0.013 to 0.020 cm. Specimens with an area of approximately 6.50 cm² were cut, polished through 4/0 abrasive paper, degreased, weighed, and their geometric surface area determined. The compositions of the alloys used in this study are presented in Table 2, "Evaporation of Types 304, 316, and 446 Stainless Steels, Inconel, INOR-8, and Haynes Alloy No. 25," this report.

Evaporation Apparatus

The two types of evaporation apparatus employed are illustrated schematically in Fig. 1. The first permitted continuous measurement of the evaporation rate by observing the weight change of a specimen suspended from a calibrated steel spring. The springs were made by winding 0.127-mm music wire around a graphite rod 127 mm in diameter and austenizing at 820°C in argon for 30 min. Following a water quench, the wire was tempered at 200°C for a period of 4 hr. The springs were cut to length and calibrated in vacuum over a weight range of 0.2500 to 1.2500 g. Spring constants varied from 1.68 to 1.90 mg/mm. Changes in the spring length were measured with a cathetometer sensitive to 0.001 mm.

The vacuum system was constructed principally of Pyrex with high-fired mullite used in the hot zone and silver-coated surfaces in the

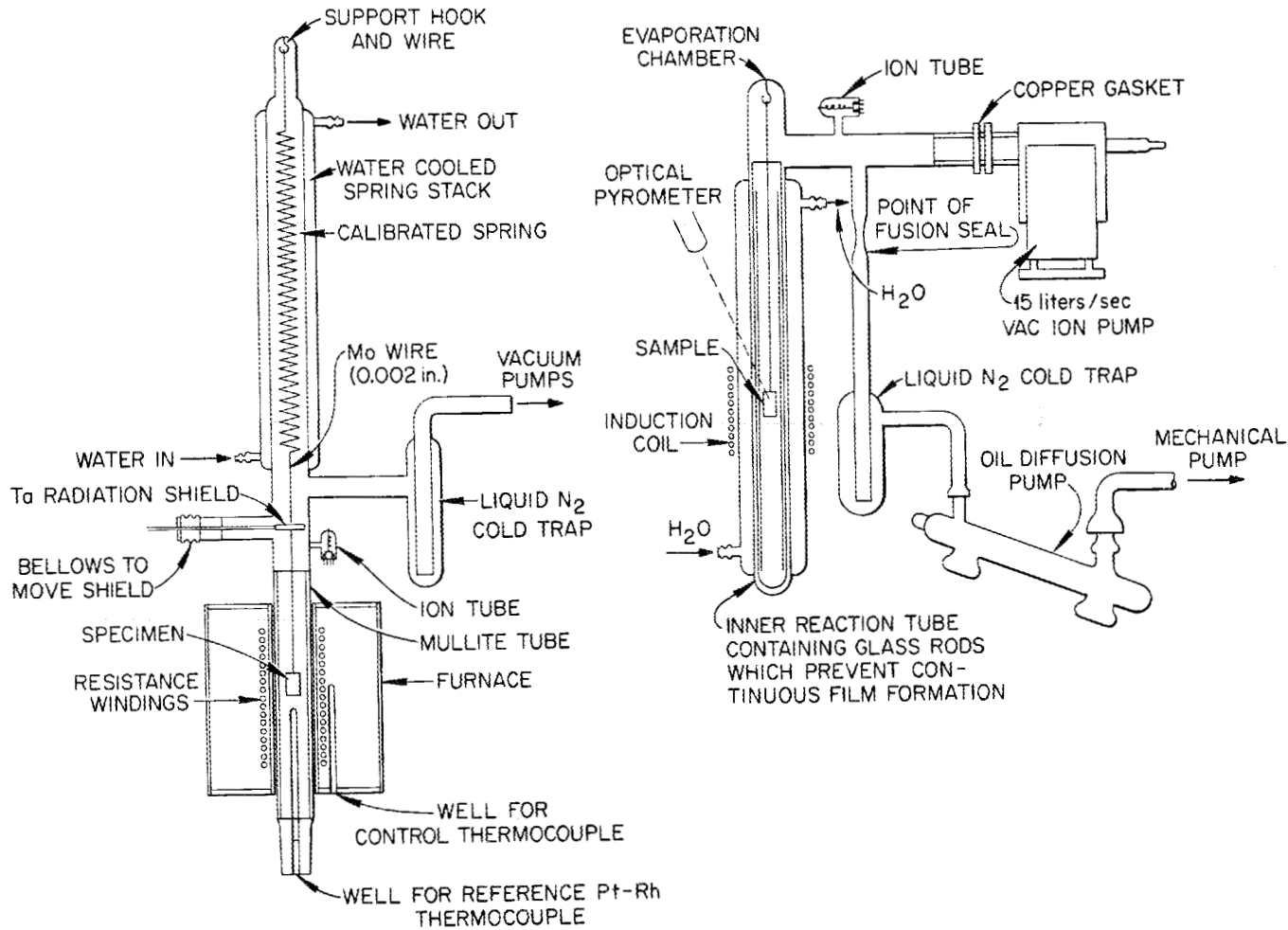


Fig. 1. Schematic Diagrams of Evaporation Systems Used in the Vaporization Studies of Iron-, Nickel-, and Cobalt-Base Alloys.

liquid-nitrogen cold traps. The vacuum pumping equipment was composed of a CVC GF-25-w Pyrex diffusion pump backed by a 1/4-hp mechanical pump. A brass bellows was placed between the diffusion pump and mechanical pump to reduce vibrational interference to the spring. The spring was also protected from thermal effects by water cooling the spring stack and inserting a tantalum radiation shield above the furnace hot zone.

Normal high vacuum techniques were followed. These included bake-out of the Pyrex at 200 to 400°C and the mullite at 1000°C, elimination of all valves and greased joints from the high vacuum side of the system, and use of liquid-nitrogen cold traps, a small system volume, and Dow Corning 704 diffusion pump oil. A base pressure of 5×10^{-8} torr was achieved at 900°C; and during the course of a test, the pressure was further decreased due to the gettering action of the metal vapors.

The second apparatus permitted the collection of the metal vapors from individual induction-heated specimens held at temperature for various periods of time. Evaporation rates of individual elements from the base alloy were determined by chemical analysis of the deposits.

The vacuum system was constructed of Pyrex and the evaporation chamber, which was water cooled, contained a replaceable inner Pyrex tube on which the vapor deposits were collected. To the inner surface of this tube were fused three 1/8-in.-diam Pyrex rods that prevented the formation of a continuous vapor-deposited film and thereby prevented induction heating of the film. A vapor deposit weighing 45.5 mg and illustrating this technique is presented in Fig. 2.

The vacuum pumping equipment consisted of a 15 liter/sec VacLion pump which was used after the system had been "roughed" to 10^{-4} torr with a cold trap-diffusion pump-mechanical pump combination. Again, normal high vacuum techniques were employed which resulted in a base pressure of 1×10^{-9} torr at 900°C.

Procedure

Once the systems had been baked out and were considered clean, the testing procedure was virtually the same for both of the systems. The systems were backfilled with dry, high-purity argon (99.998%) to

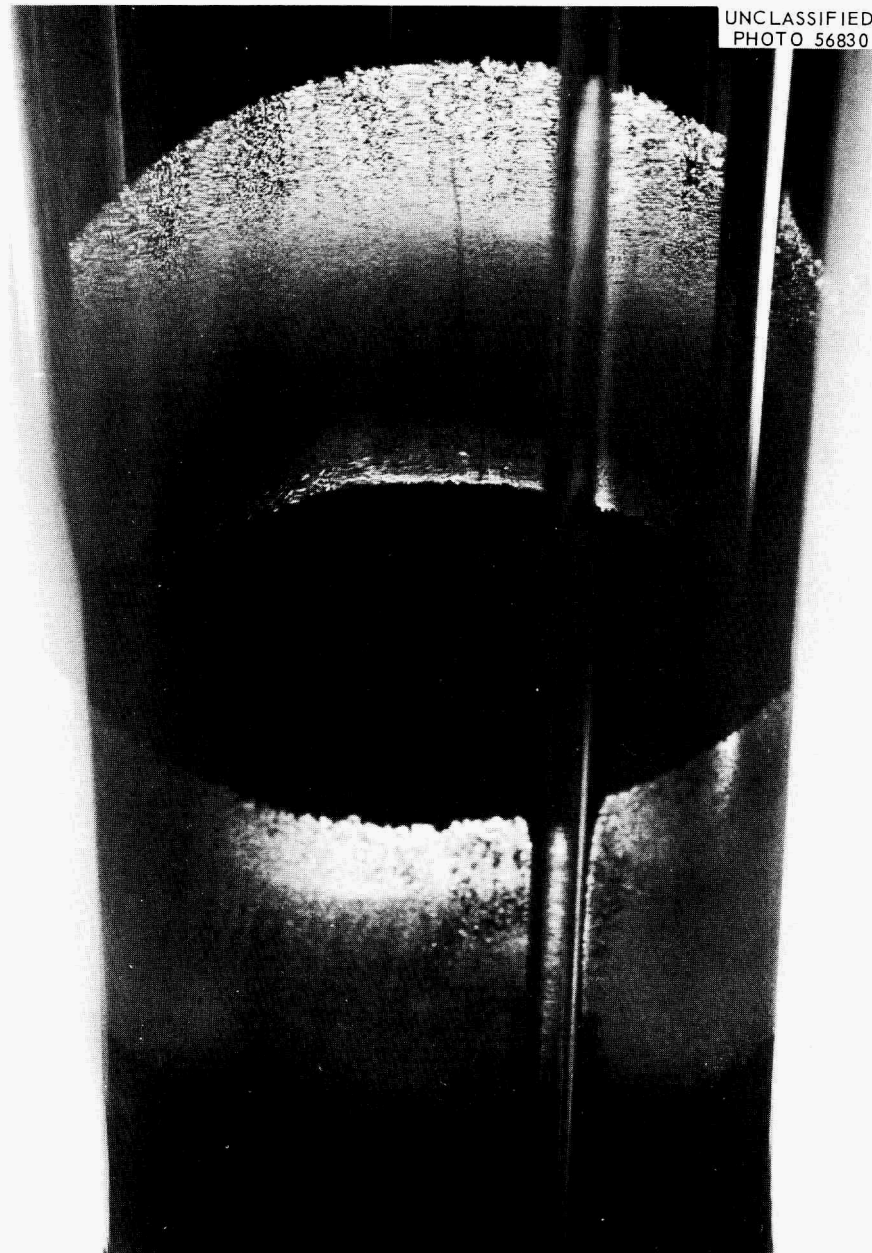


Fig. 2. Vapor Deposits from a Type 316 Stainless Steel Specimen with Discontinuities which Prevent Film Heating in an Induction Field.

atmospheric pressure, opened, and loaded with the desired specimens. The systems were resealed and immediately evacuated; the entire procedure required approximately 15 to 20 min. When a pressure of 10^{-7} torr was obtained, heat was applied to the specimens at a rate which did not increase the pressure to above 10^{-6} torr. Under these conditions, a 24-hr period was required to bring the specimen to the desired temperature.

Evaporation tests were conducted on types 304 and 446 stainless steels, Inconel, INOR-8, and Haynes alloy No. 25 at 872 and 982°C for times up to 700 hr. Type 316 stainless steel was tested at 760, 872, 927, and 982°C for times up to 3500 hr.

RESULTS AND DISCUSSION

Validity of the Experimental Technique

The accuracy of the experimental technique used in this investigation was verified by determining the vapor pressure of pure iron and nickel using the Knudsen-Langmuir equation with the vaporization coefficient equal to unity. The vapor pressures determined by this technique agreed quite well with the published values. In the case of nickel, the experimental value of 2.25×10^{-7} torr is compared with the published value² of 3.00×10^{-7} torr at 1038°C, while for iron an experimental value of 1.54×10^{-7} torr is compared to a published value³ of 1.77×10^{-7} torr at 872°C. The results of these evaporation tests, illustrated in Fig. 3, show a linear weight loss with time, a behavior characteristic of pure metals.³

Metallographic examination showed that the surfaces of these metals became faceted after exposure to high vacuum at elevated temperatures, as illustrated by the pure nickel specimen shown in Fig. 4. The cross-sectional microstructure, illustrated in Fig. 5, showed grain boundary evaporation; however, no grain boundary grooving at the surface occurred in tests to 915 hr.

²J. F. Elliott and M. Gleiser, Thermochemistry for Steelmaking, Vol. 1, p. 270, Addison-Wesley, Reading, Mass., 1960.

³E. A. Gulbransen and K. F. Andrew, Trans. Met. Soc. AIME 221, 1247 (1961).

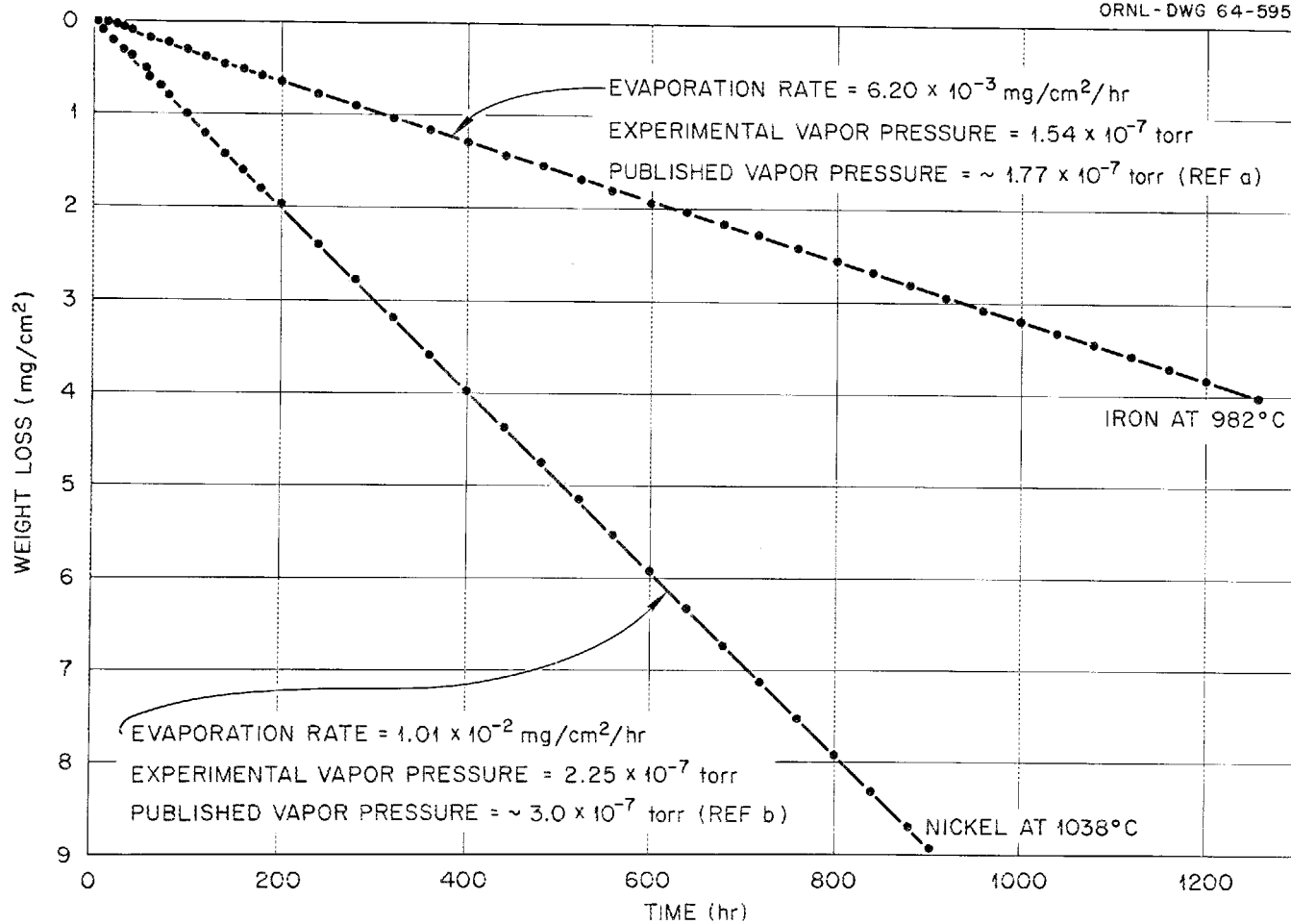


Fig. 3. Evaporation of Iron and Nickel at 982 and 1038°C, Respectively.
Refs: (a) J. F. Elliott and M. Gleiser, Thermochemistry for Steelmaking, Vol. 1, p. 270, Addison-Wesley, Reading, Mass., 1960. (b) E. A. Gulbransen and K. F. Andrew, Trans. Met. Soc. AIME 221, 1247 (1961).

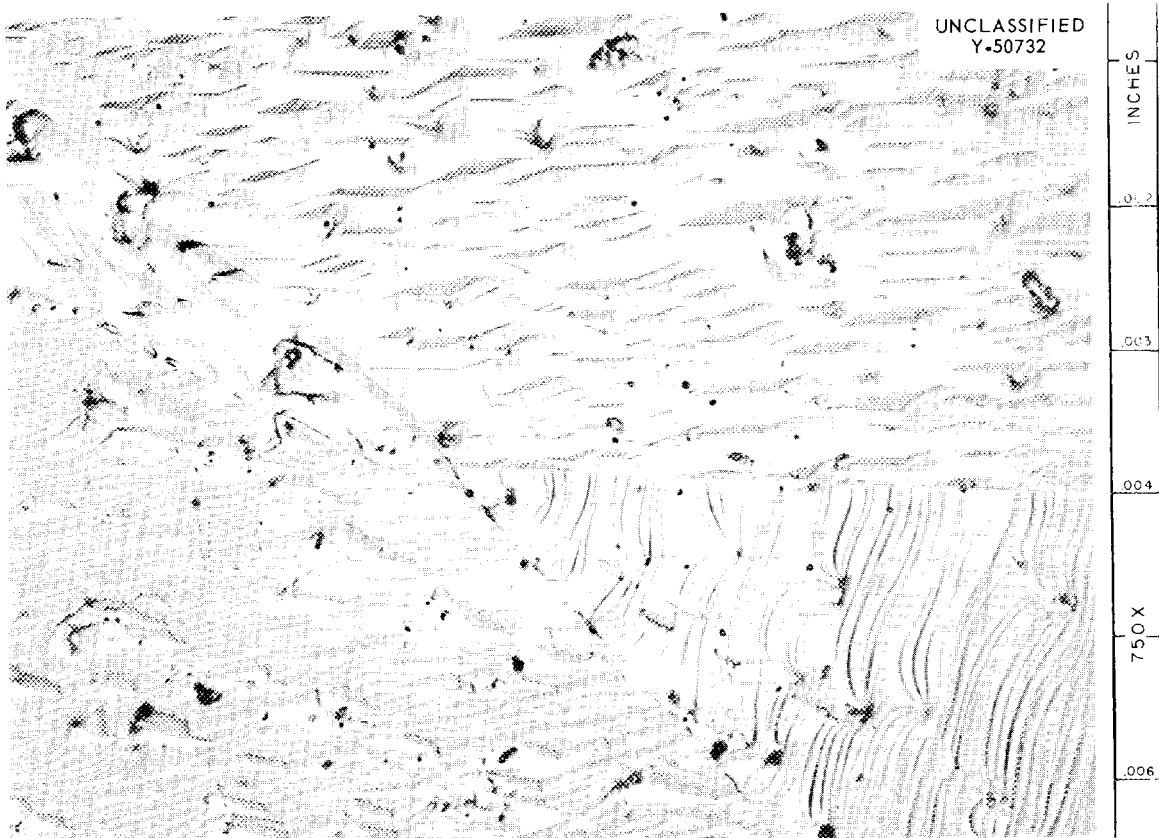


Fig. 4. Evaporated Surface of High-Purity Nickel Evaporated at 1038°C and 5×10^{-8} torr for 915 hr. 750X

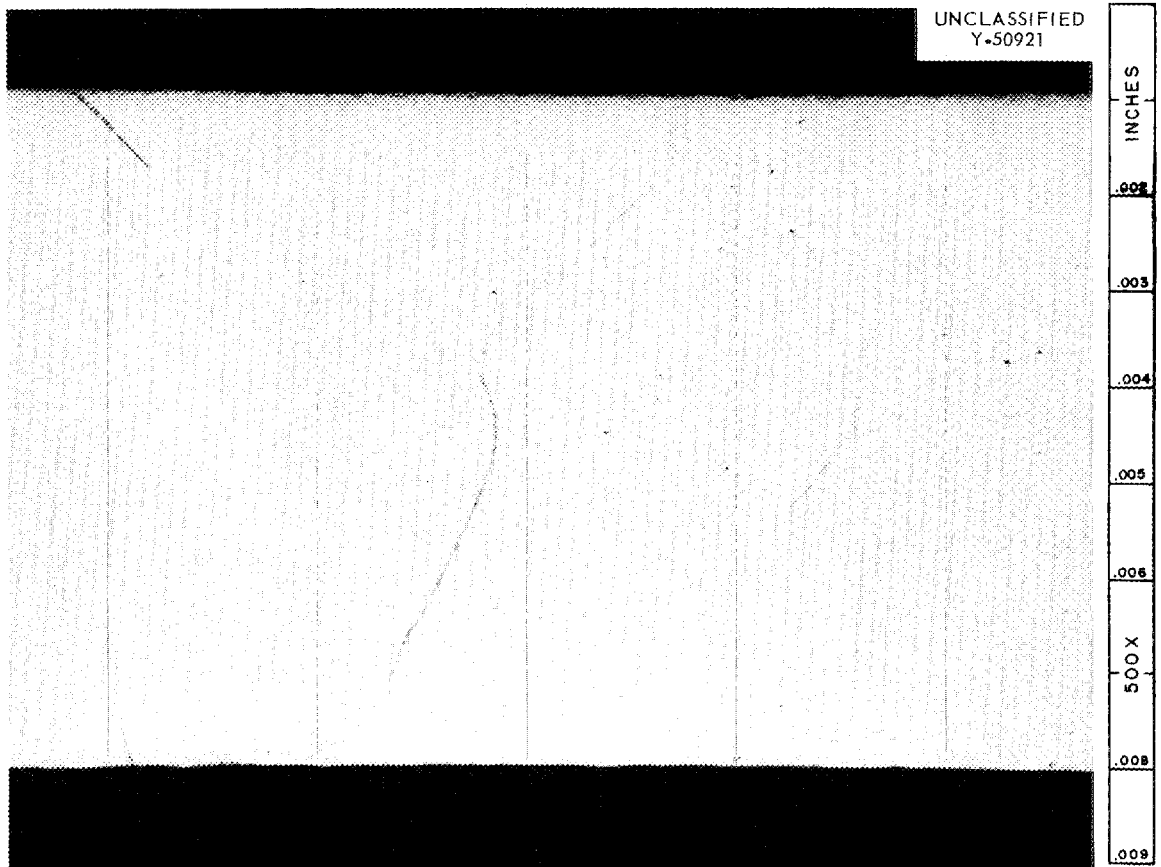


Fig. 5. Cross Section of High-Purity Nickel Evaporated at 1038°C and 5×10^{-8} torr for 915 hr. Etchant: 70% CH_3COOH -29.5% HNO_3 -0.5% HCl . 500X

Evaporation of Types 304, 316, and 446 Stainless Steels,
Inconel, INOR-8, and Haynes Alloy No. 25

Polished Surfaces

Evaporation losses from types 304, 316, and 446 stainless steels, Inconel, INOR-8, and Haynes alloy No. 25 were measured at 872 and 982°C and at pressures ranging from 5×10^{-7} to 5×10^{-8} torr. The results of short-term (to 700 hr) tests, summarized in Table 2, indicated that the evaporation rates at both temperatures increased with increasing chromium and probably increasing manganese concentrations. Further, the rates at any given temperature were not constant but decreased with time. The magnitude of the decrease was less with increasing temperature and generally with decreasing chromium content.

The curves illustrated in Fig. 6 compare the continuous evaporation losses of these alloys at 872 and 982°C, respectively. From these data it appears that the evaporation rates became nearly constant after approximately 50 hr. As will be shown later, much longer tests with type 316 stainless steel (and probably other alloys containing high chromium concentrations) indicated that the evaporation rate actually continues to decrease slowly with time.

The initial evaporation losses, which came primarily from the surfaces, resulted in severe changes in surface concentration of the higher vapor pressure elements, particularly at 872°C. At 982°C the diffusion rates of the various elements were rapid enough to replenish surface losses. For example, results of several microprobe analyses showed that at 872°C manganese and chromium concentration gradients existed at the conclusion of several 600-hr tests, while at 982°C the concentration gradients were barely detectable.

A second source of evaporative losses is the edges of the surface grains.⁴ Metallographic examination showed that annealing for 1 hr at 900 to 1000°C resulted in grain boundary grooving.

⁴W. L. Winterbottom and J. P. Hirth, Evaporation of Silver Crystals, pp. 16-18, Carnegie Institute of Technology, Metals Research Laboratory, 1962.

Table 2. Evaporation Rates of Iron-, Nickel-, and Cobalt-Base Alloys at 5×10^{-7} to 5×10^{-8} torr

Alloy	Alloy Composition (wt %) ^a									Evaporation Rate (mg/cm ² /hr) $\times 10^{-4}$			
	Fe	Ni	Mo	Co	C	W	Mn	Si	Cr	872°C		982°C	
										Initial ^b	Final ^c	Initial	Final
INOR-8	5.10	69.76	17.81	0.15	0.04		0.29	0.58	6.78	1.54	1.54	30.8	30.8
Inconel	5.84	79.62			0.04		0.54		14.29	7.57	2.89	59.7	33.5
Type 316 stainless steel	64.03	13.28	2.25		0.05		1.67	0.74	17.05	30.0	6.59	114.0	66.4
Type 304 stainless steel	68.84	10.68			0.07		1.61	0.84	18.04	53.7	6.71		
Haynes alloy No. 25	1.41	10.50		49.81	0.02	15.72	1.58	0.76	19.46	58.5	5.66	140.0	69.2
Type 446 stainless steel	73.91	0.71			0.02		1.20	0.14	24.71	73.8	25.7	156.0	69.0

^aImpurity elements not listed.

^bMaximum rate during first 50 hr of test.

^cRate during last 50 hr of test.

UNCLASSIFIED
ORNL-DWG 63-4370

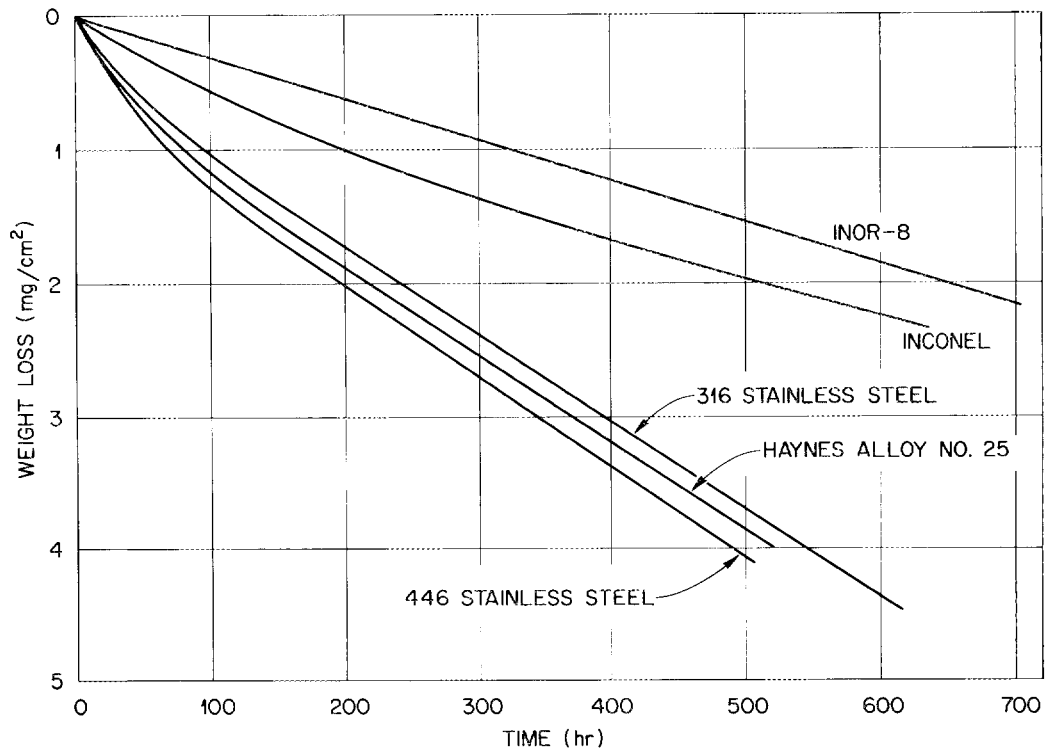
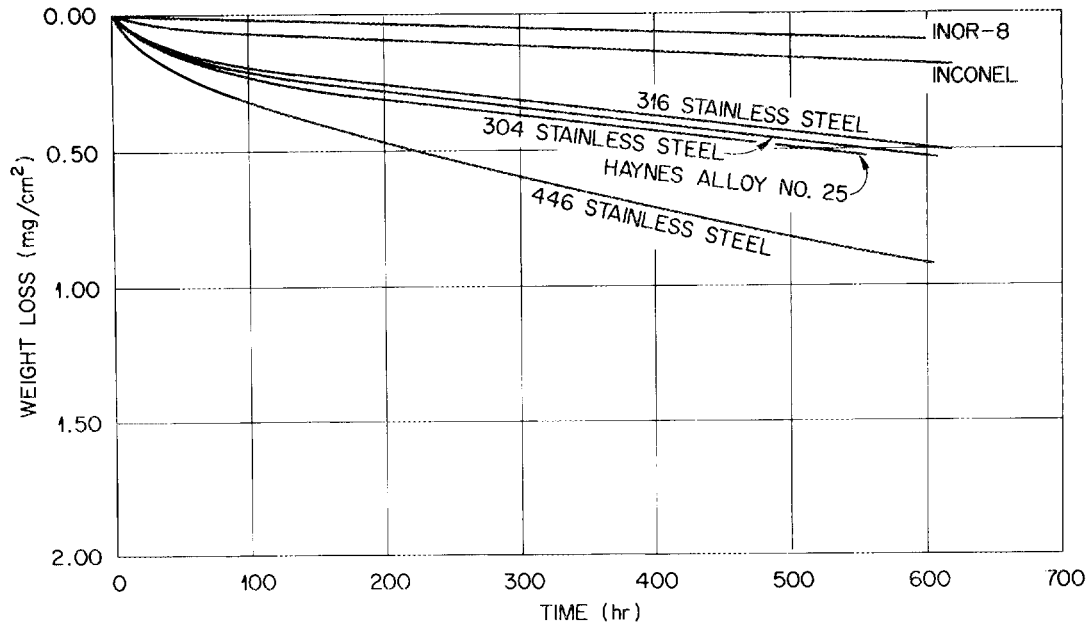


Fig. 6. Evaporation Losses of Iron-, Nickel-, and Cobalt-Base Alloys at 872 and 982°C and Approximately 5×10^{-7} to 5×10^{-9} torr.

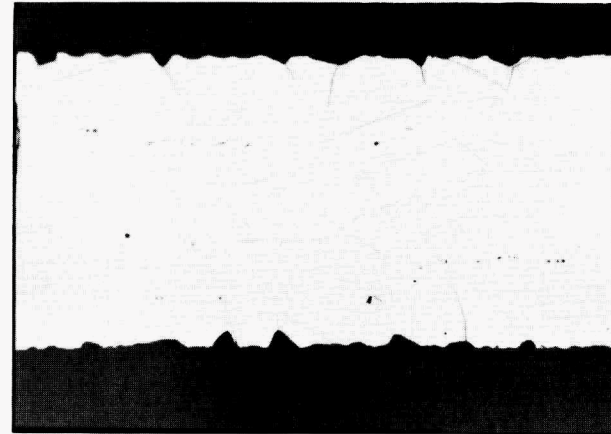
During the later stages of evaporation when the curves illustrated in Fig. 6 approached linearity, the grain boundaries beneath the surface exhibited severe material losses, subsurface voids appeared, precipitates near the surface decreased, and grain growth resulted — probably from loss of carbon. These evaporation effects to 700 hr at 982°C are metallographically illustrated in Fig. 7.

Analytical results of the pre- and posttest alloy compositions revealed substantial losses of chromium, manganese, and carbon. The results of several 600-hr tests are summarized in Table 3. The manganese and chromium losses increased with increasing chromium and manganese concentration in the original alloy because of their higher vapor pressures, while the carbon losses did not vary substantially. This behavior and the fact that metallographic examination revealed bands near the specimen surfaces which were depleted of precipitates suggested a decomposition of carbides.

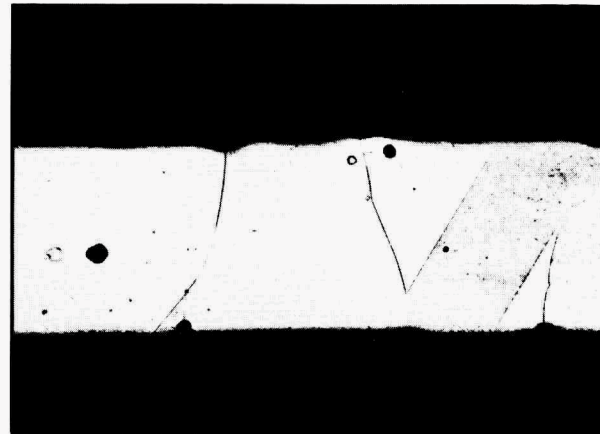
Table 3. Elemental Losses of Iron-, Nickel-, and Cobalt-Base Alloys Evaporated at 872°C

Alloy ^a	Length of Test (hr)	Percent Decrease in Original Concentration		
		Mn	Cr	C
INOR-8	598	13.9	1.61	29.7
Inconel	618		3.86	28.5
Type 316 stainless steel	604	21.6	5.21	27.4
Type 304 stainless steel	608	29.4	5.96	27.1
Haynes alloy No. 25	557	44.9	3.01	28.4
Type 446 stainless steel	613	54.1	4.85	12.1

^aSee Table 2 for original composition.

UNCLASSIFIED
Y-51004

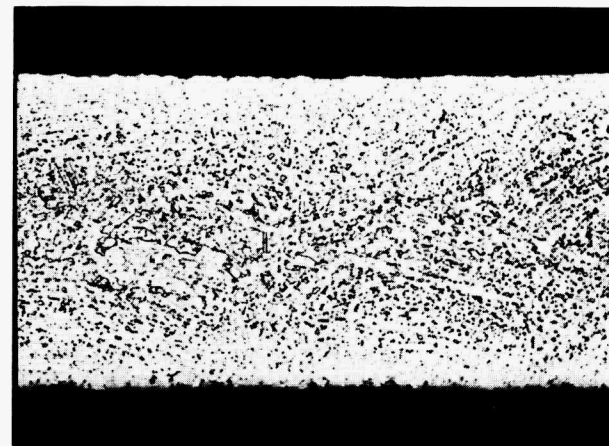
INOR-8



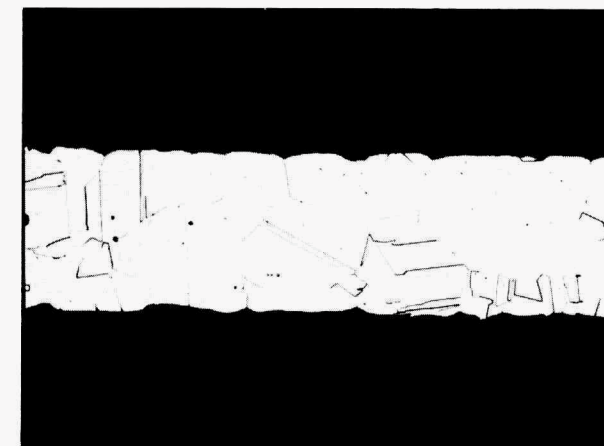
INCONEL



TYPE 316 STAINLESS STEEL



HAYNES ALLOY NO. 25



TYPE 446 STAINLESS STEEL

Fig. 7. Cross-Sectional Microstructures of Iron-, Nickel-, and Cobalt-Base Alloys Illustrating Evaporation Effects at 982°C and 5×10^{-7} to 5×10^{-8} torr. Etchant: glyceria regia. 500X

Oxidized Surfaces

It has been demonstrated that surface oxides will retard the evaporation of pure base metals.⁵ To ascertain the effect of an oxide film on the present alloys, several specimens were oxidized in air and subsequently evaporation tested. The oxidizing conditions, oxide identification, and results of subsequent evaporation tests at 982°C are summarized in Table 4. The postevaporation x-ray data indicated that only Cr₂O₃ was stable under the test conditions. Comparison of initial and final evaporation rates for INOR-8 and type 316 stainless steel showed that the complex oxide compositions did initially retard evaporation of the base metal. In the case of Inconel, it is postulated that the greater initial rate is due to decomposition of unknown oxides which were present in quantities too small to be detected by normal x-ray procedures. The weight loss versus time plot was virtually a straight line, and only on an expanded scale was the initial higher rate obtainable. In the case of Haynes alloy No. 25, it is believed that the high initial evaporation rate is due to the rapid vacuum decomposition of the cobalt-bearing oxides.

This general type of behavior suggested the existence of a transition period during which time the oxide film was evaporating without exposure of the base metal. When portions of the base metal became exposed, the evaporation rates were accelerated and for short-term tests (500 to 700 hr) appeared to be linear. Metallographic examination showed that the oxide film initially deteriorated at the intersection of the surface and the grain boundaries and that the subsequent evaporation losses came principally from the grain boundaries.

Comparison of the evaporation rates (Tables 2 and 4) for both the polished and oxidized conditions of the alloys investigated indicates that the oxide remaining on the surface continued to retard evaporation from grain faces. For example, the final evaporation rates of INOR-8, Inconel, type 316 stainless steel, and Haynes alloy No. 25 at 982°C were

⁵Ibid.

Table 4. The Effect of Air Oxidation on the Subsequent Evaporation Rates of Various Alloys at 982°C

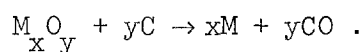
Alloy	Oxidation			X-Ray Identification of Oxide Film	Duration of Test (hr)	Evaporation Rate (mg/cm ² /hr) × 10 ⁻⁴		Oxide Present after Evaporation
	Temperature (°C)	Time (hr)	Oxygen Pickup (mg/cm ²)			Initial ^a	Final ^b	
INOR-8	870	50	0.0521	NiMoO ₄ + NiCr ₂ O ₄ + Cr ₂ O ₃ + NiFeO ₄	531	8.5	25.0	none
Inconel	980	25	0.1735	Cr ₂ O ₃	522	36.3	30.5	Cr ₂ O ₃
Type 316 stainless steel	980	100	4.3950	αFe ₂ O ₃ + NiO·Fe ₂ O ₃ + 3Fe ₂ O ₃ ·Cr ₂ O ₃	504	1.94	6.65	Cr ₂ O ₃ + Fe ₃ O ₄ (trace)
Haynes alloy No. 25	1038	90	0.0229	Cr ₂ O ₃ + NiO·Fe ₂ O ₄ + CoFe ₂ O ₄ + Co ₂ MnO ₄	510	66.5	3.34	Cr ₂ O ₃ + αFe ₃ O ₄ (trace)

^aMaximum rate during initial 50 hr of test.

^bRate during last 50 hr of test.

reduced by factors of 1.2, 1.1, 10, and 21, respectively, when oxidized in air. As will be discussed subsequently, longer term tests on oxidized type 316 stainless steel indicated a diminution of protection with time.

The evaporation data of oxidized specimens indicated that oxide thickness as well as its composition may be instrumental in retarding evaporation of the base metal. In addition, the carbon content of the base metal may have influenced the rate at which surface oxides deteriorated in vacuum at elevated temperatures in accord with the following reaction.



For example, the oxygen pickup in type 316 stainless steel was 4.395 mg/cm² when oxidized in air at 980°C for 100 hr. At 982°C this specimen exhibited initial and final evaporation rates of 1.94 and 6.65 × 10⁻⁴ mg/cm²/hr, respectively. A comparison of x-ray intensities of this heavily oxidized specimen placed the amount of oxygen in the form of Cr₂O₃ (Table 4) at approximately 20% or 0.879 mg/cm². These data can be compared with evaporation data obtained from specimens oxidized in low-pressure wet hydrogen at 870°C for 170 hr to produce only Cr₂O₃ on the surfaces. The evaporation results of these specimens showed, for example, that an oxygen pickup of 0.2804 mg/cm² yielded initial and final evaporation rates of 26.9 and 35.7 × 10⁻⁴ mg/cm²/hr, respectively (see Table 7). It is postulated that the thinner Cr₂O₃ film formed in wet hydrogen decomposed more rapidly because of carbon reductions and thereby resulted in a greater evaporation rate of the type 316 stainless steel base metal at the grain boundaries.

For Haynes alloy No. 25 that was oxidized in air at 1040°C for 90 hr, an oxygen pickup of 0.0229 mg/cm² resulted in initial and final evaporation rates of 66.5 and 3.34 × 10⁻⁴ mg/cm²/hr, respectively. In addition to the rapid decomposition of the cobalt-bearing oxides leaving only Cr₂O₃ on the surface, it may also be noted that the original Haynes alloy contained only 0.02 wt % C and this may have been somewhat reduced by air oxidation. Both of these factors could have contributed to the relatively low final evaporation rate of this alloy.

Evaporation of Type 316 Stainless Steel

Polished Surfaces

Short-term tests (500 to 650 hr) conducted at 982, 927, 872, and 760°C indicated that the initial evaporation rates at all temperatures were greater than the final rates; and as the test temperature was lowered, the difference between the initial and final rates increased. Further, the time necessary to achieve a significant decrease in evaporation rate increased with decreasing temperature. For present purposes this time is defined as the transient period. This behavior suggests the development of concentration gradients of the evaporating elements in the specimens. If this reasoning is correct, then long-term tests at all the test temperatures should show a constantly decreasing evaporation rate.

To substantiate this hypothesis, tests exceeding 1000 hr were conducted and the results are compared to the shorter term data in Table 5. The long-term test data indicated that at all temperatures the evaporation rates continued to decrease with time. This phenomenon was more acutely demonstrated at 872 and 760°C. For example, the data at 872°C showed that at 50 hr the rate was 2.68×10^{-3} mg/cm²/hr, while at 610 and 3400 hr the rate had decreased to 6.38 and 3.90×10^{-4} mg/cm²/hr, respectively. A typical concentration gradient for manganese and chromium, as determined by a microprobe analysis, is shown in Fig. 8.

The data at all of the temperatures investigated can be represented by curves of the type

$$\Delta W = At^B$$

where A and B are constants. At 872°C the experimental data can be represented by the equation

$$\Delta W = 0.0068 t^{0.68} \tag{1}$$

or its equivalent form

$$\log \Delta W = 0.68 \log t - 2.17 \tag{2}$$

where

$$\Delta W = \text{weight loss in mg/cm}^2; t = \text{time in hours.}$$

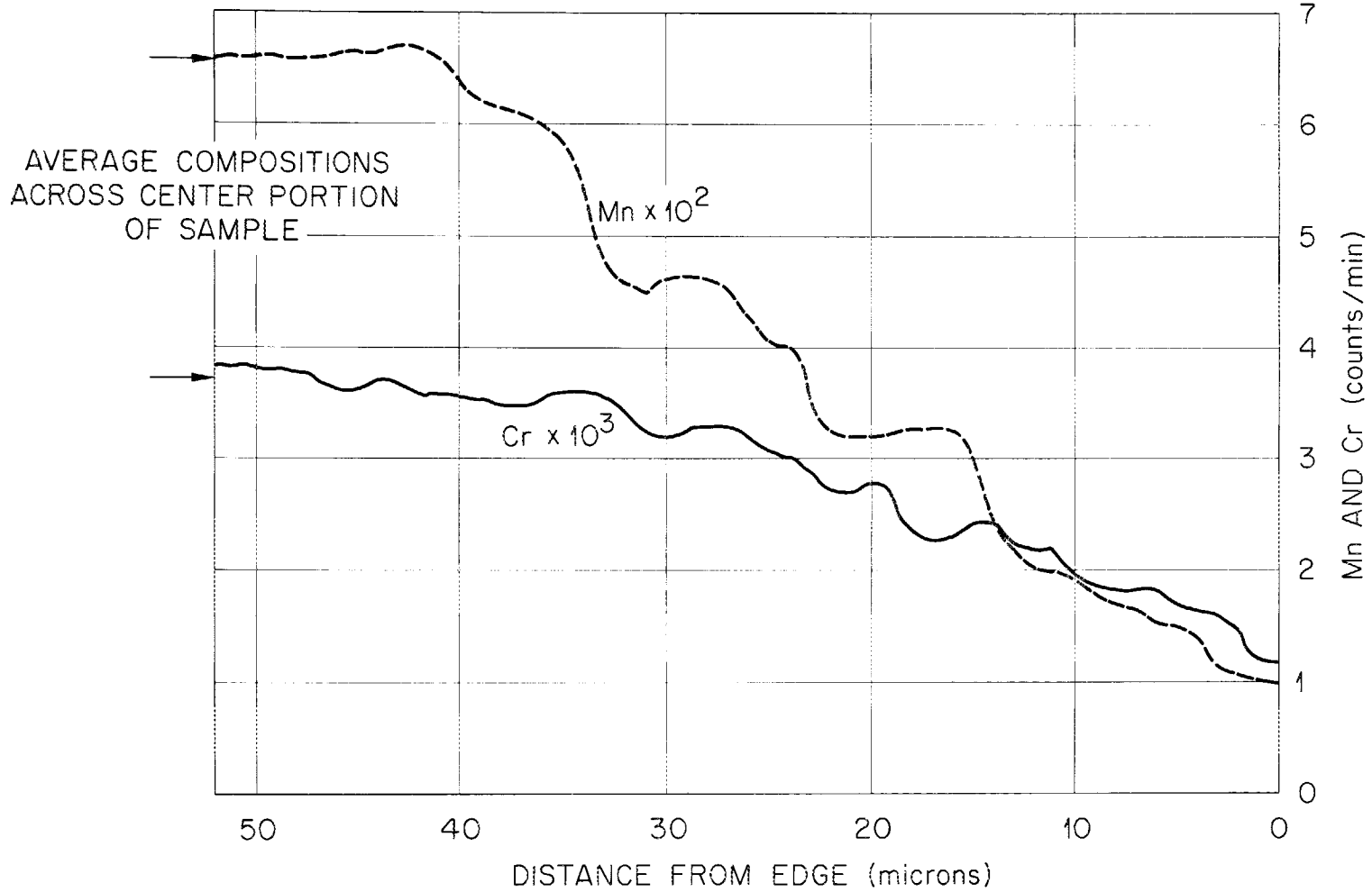


Fig. 8. Microprobe Traverse of Type 316 Stainless Steel Heated at 872°C in a Vacuum of 5×10^{-8} torr for 598 hr.

Table 5. Evaporation Rates and Length of Transient Periods of Type 316 Stainless Steel as a Function of Temperature

Testing Temperature (°C)	Short-Term Tests			Long-Term Tests				
	Test Duration (hr)	Evaporation Rate (mg/cm ² /hr) × 10 ⁻⁴		Test Duration (hr)	Evaporation Rate (mg/cm ² /hr) × 10 ⁻⁴		Average Length of Transient Period (hr)	Decrease from Initial to Final Evaporation Rate (%)
		Initial ^a	Final ^b		Initial	Final		
982	616	114.0	66.4	956	120.0	65.9	30	45
927	598	39.8	21.9	1832	42.3	20.5	50	52.6
872	613	30	6.59	3453	26.8	3.9	80	85.4
760				1321	6.56	0.528	200	93

^aMaximum rate during initial 50 hr of test.

^bRate during final 50 hr of test.

The first derivative of Eq. (1) gives the instantaneous vaporization rate in milligrams per square centimeter per hour at 872°C.

$$\frac{d\Delta W}{dT} = 0.0046 \left(t^{-0.322} \right). \quad (3)$$

The evaporation losses in the form of Eq. (2) are presented graphically for the various temperatures in Fig. 9. Some deviation may be noted for small times at the lower temperatures.

Chemical analyses of the deposited metal vapors from tests conducted at 7.0×10^{-9} torr and 872°C are summarized in Table 6 and presented graphically in Fig. 10. Manganese initially is the major contributor to the total evaporation rate, but longer tests have shown that chromium losses increase while manganese losses decrease. The losses of Si, Fe, and Ni also increase while carbon losses decrease with time. These results indicate a selective loss of alloying elements, resulting in a constantly changing surface composition at temperatures of 872°C or lower. At 927 and 982°C, there was no detectable evidence of concentration gradients, indicating greater bulk diffusion of the alloying elements, thereby accounting for the smaller difference between the initial and final evaporation rates.

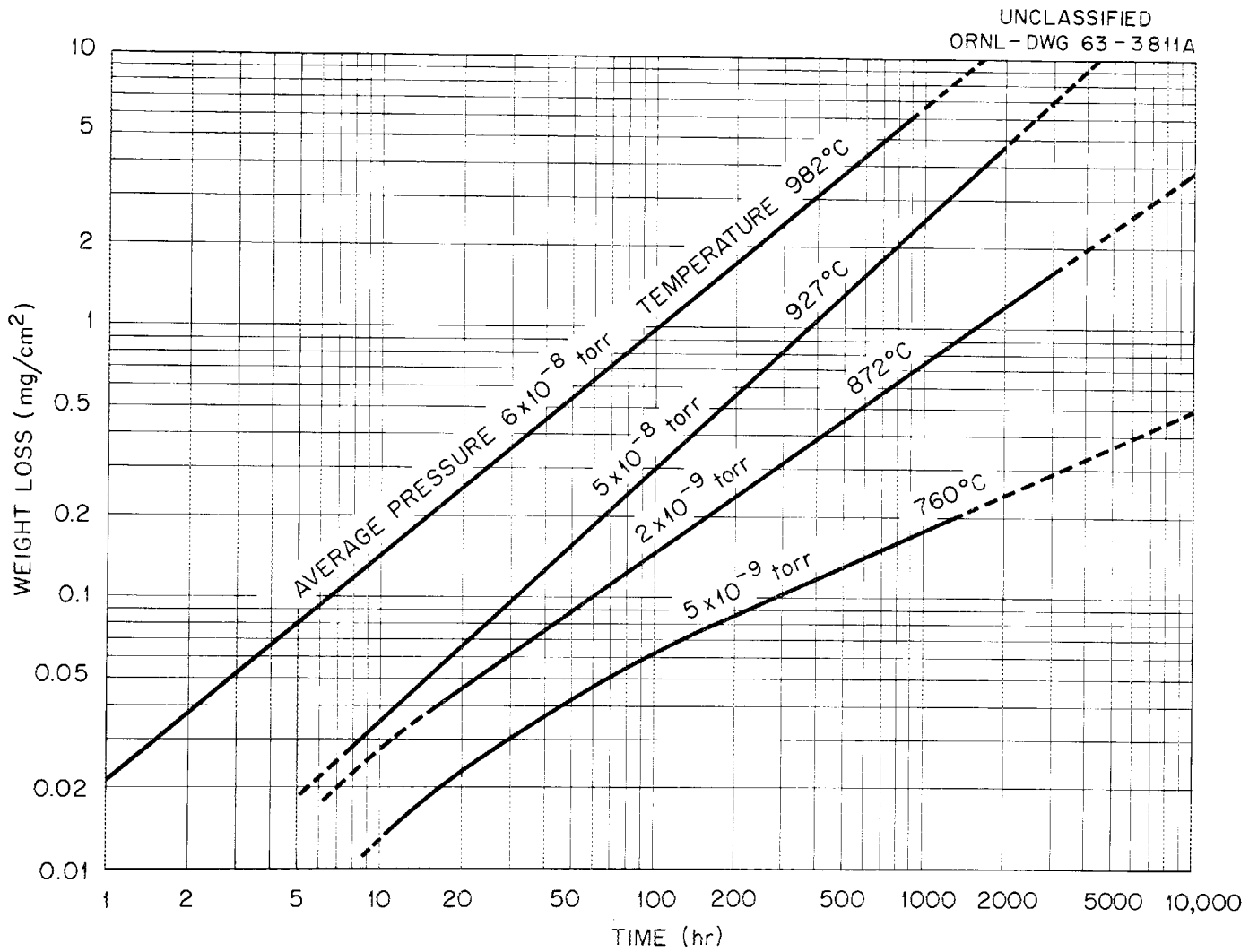


Fig. 9. Evaporation Losses of Type 316 Stainless Steel in the Polished Condition.

Table 6. Chemical Analyses of Deposits Evaporated from
Type 316 Stainless Steel at 872°C and 7×10^{-9} torr

Element	Vapor Pressure of Element (torr)	Analyses ^a of Original Alloy (wt %)	Analyses of Vapor Deposit at Various Times (wt %)						Ratio: Weight Percent Deposit/Weight Percent Alloy					
			(hr)						(hr)					
			6	12	25	50	150	480	6	12	25	50	150	480
Mn	8×10^{-4}	1.67	77.72	71.24	70.2	68.1	59.85	50.88	46.5	42.7	42.0	40.8	35.8	30.9
Cr	2.5×10^{-6}	17.05	3.18	3.84	4.40	7.91	19.95	29.4	0.187	0.225	0.258	0.464	1.17	1.723
Si	7×10^{-7}	0.74	0.712	0.971	1.31	1.45	1.51	1.70	2.03	2.77	3.74	4.14	4.31	4.86
Fe	1.5×10^{-8}	64.03	1.29	1.33	2.39	4.86	9.03	12.27	0.020	0.020	0.037	0.075	0.141	0.192
Ni	4×10^{-9}	13.28	1.01	1.4	1.62	1.71	1.83	1.95	0.076	0.105	0.122	0.128	0.138	0.147
C	5×10^{-19}	0.05	7.53	4.32	3.93	2.11	1.70	1.41	150.6	86.4	78.6	42.2	34.0	28.2
Mo	3×10^{-14}	2.25												

^aAnalyses of impurity elements are omitted.

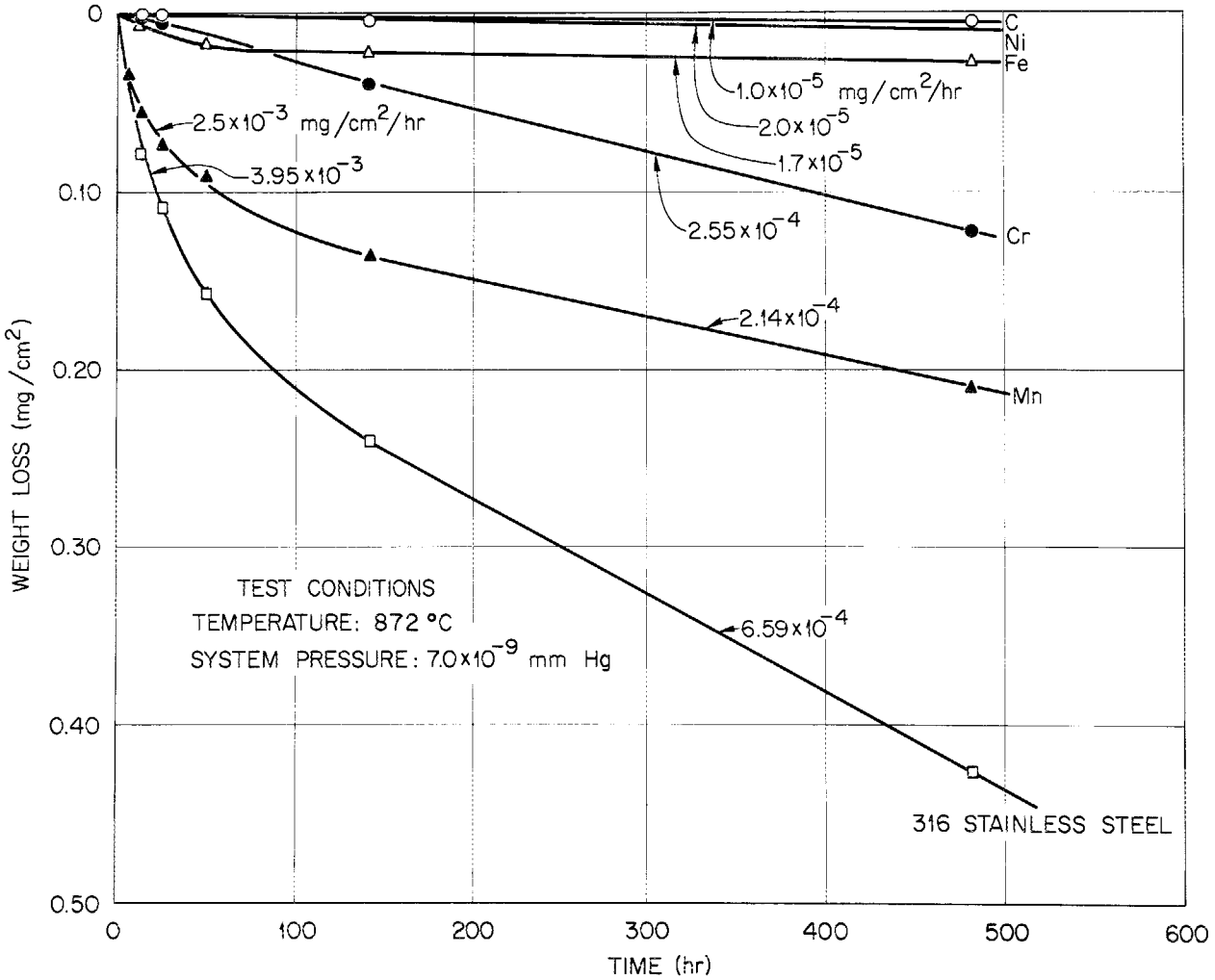


Fig. 10. Evaporation Losses of the Major Elements from Type 316 Stainless Steel at 872°C.

The microstructural manifestations of evaporation such as subsurface voids, grain growth, grain boundary grooving, and grain boundary losses were the same at all temperatures studied; however, longer times were required at the lower temperatures to produce equal magnitudes for any one type of effect. In multicomponent alloys containing high vapor pressure alloying elements and interstitial impurities, the grain boundaries become enriched in these elements and impurities. The high degree of lattice disorder existing at the grain boundaries promoted a greater evaporation rate when compared to the grains themselves. It is, therefore, concluded that initial evaporation losses from the grain boundaries exposed adjacent grain surfaces, as illustrated in Fig. 11a and b. Further evaporation from the edges of the surface grains resulted in the formation of grooves which continued to widen with time, as illustrated in Fig. 11c and d. As the grooves widened (receded across the grain) and subsurface voids continued to coalesce at the grain boundaries, the surfaces of the specimens became smoother. This was accompanied by the formation of a semicontinuous network of voids in the grain boundaries. This behavior is illustrated in Fig. 11e.

In the case of type 316 stainless steel, grain boundary grooving became apparent after 1 hr at 1000°C and 4 hr at 800°C. Other microstructural changes such as subsurface void formation, grain growth, disappearance of precipitates, ferrite formation at the specimen surfaces, and widening of the grain boundaries became readily apparent after testing times of 500 hr at 872°C. These phenomena are metallographically illustrated in Figs. 12 and 13. For test periods greater than 1000 hr, chi phase began to precipitate and severe grain boundary voids began to appear, a behavior also illustrated in Figs. 12 and 13.

When ferrite precipitation was observed metallographically, x-ray analysis verified this conclusion, and it was postulated that initially evaporation losses depleted the surface regions of austenite stabilizers (e.g., C and Mn). At 872 and 982°C, this precipitation started just prior to heavy or deep grain boundary losses, but as the specimen thickness decreased, the ferrite precipitate disappeared. It was felt that the low nickel losses coupled with high loss of chromium allowed the ferrite to retransform to γ -iron (austenite). For example, it is seen

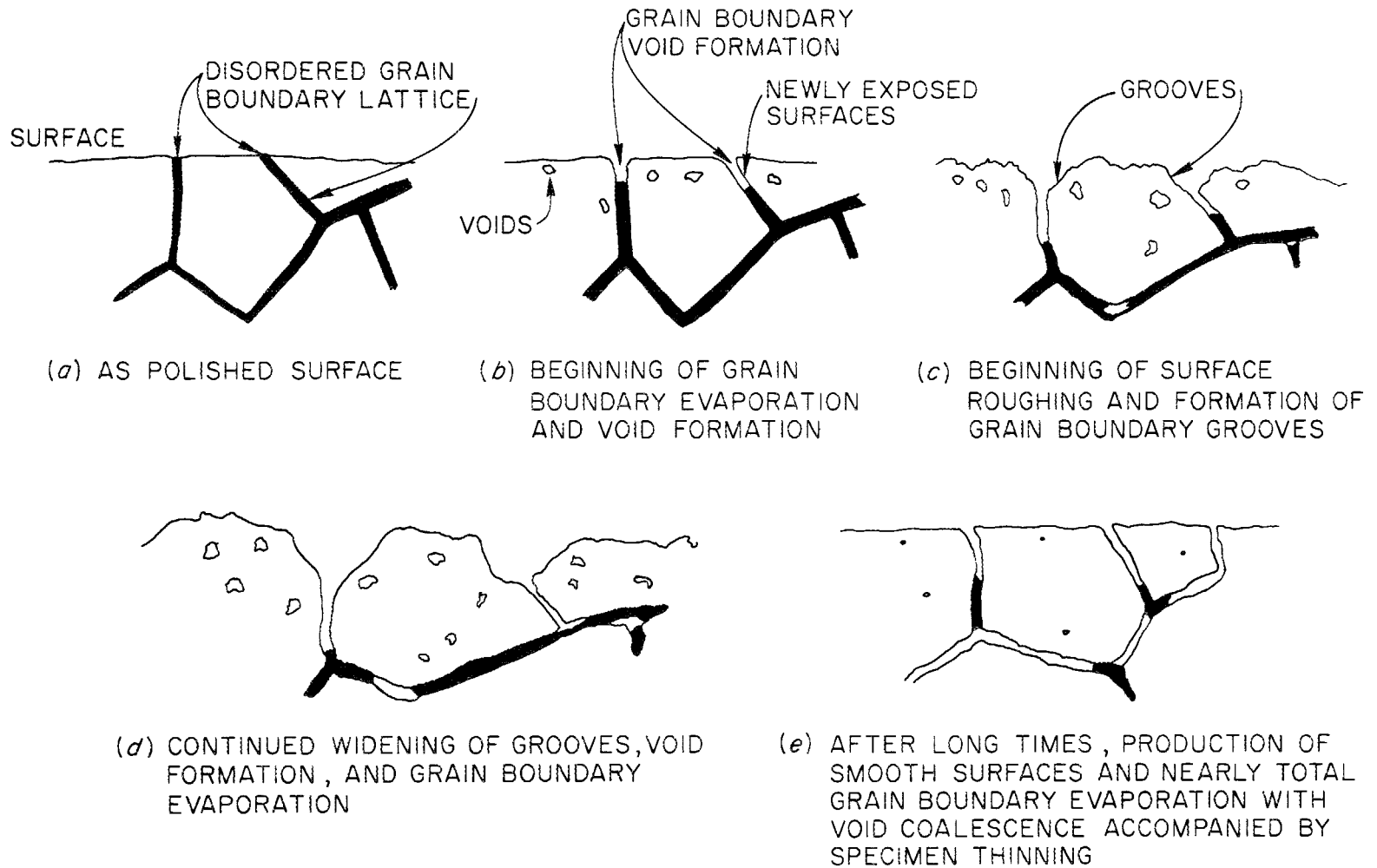
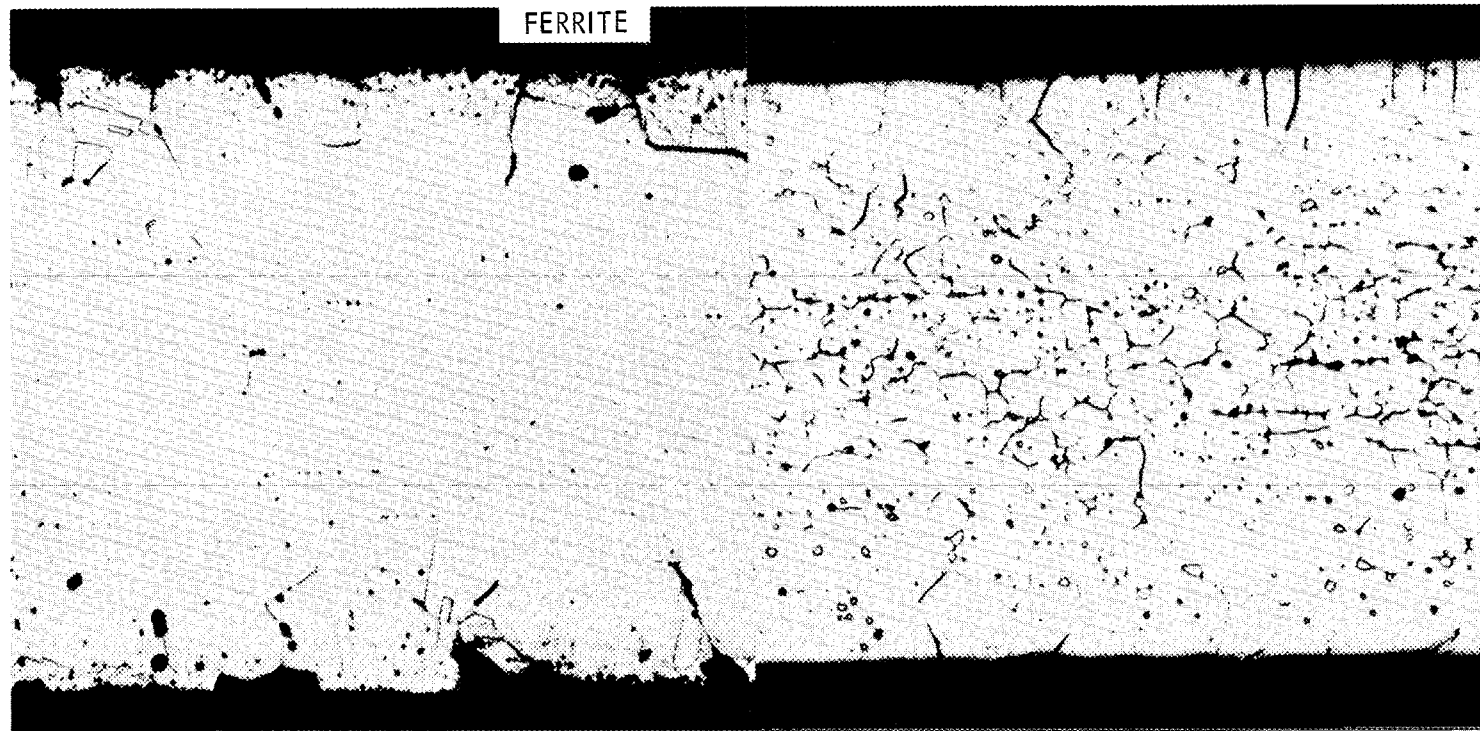


Fig. 11. Evaporation Sequence for Thin Specimens of Type 316 Stainless Steel Exposed to High Vacuum Between 800 and 1000°C.

UNCLASSIFIED
PHOTO-62803



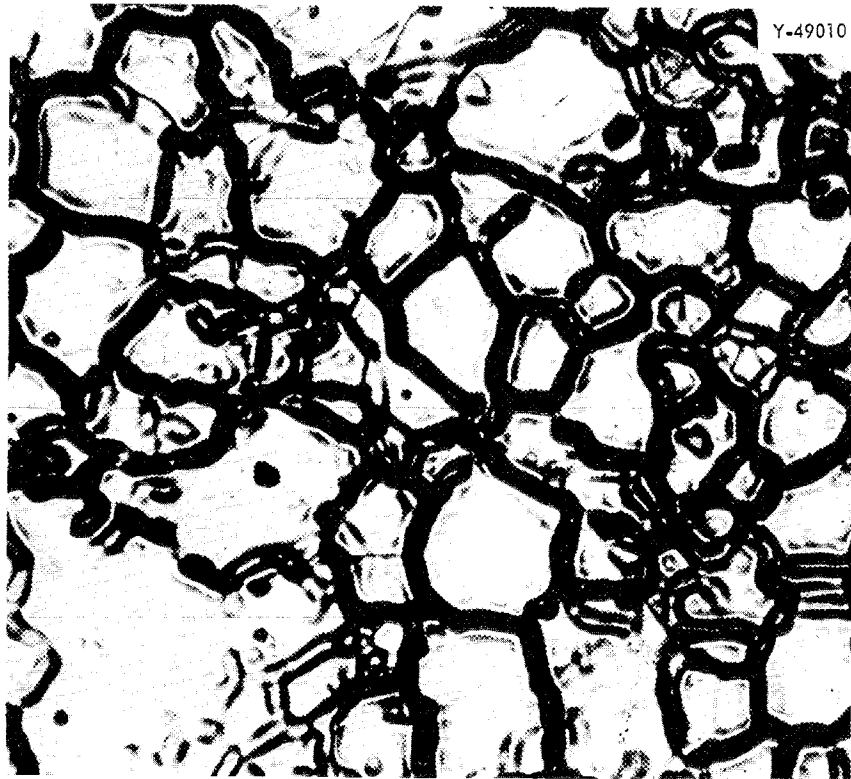
892 hr

(Y-49174)

3453 hr

(Y-50726)

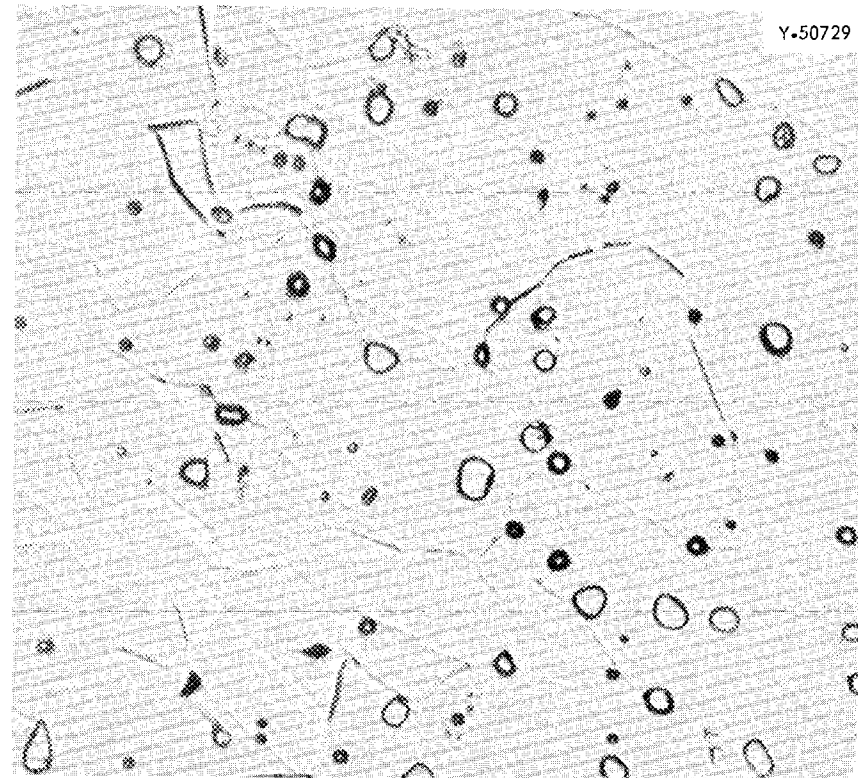
Fig. 12. Cross Section of Type 316 Stainless Steel Evaporation Tested at 872°C and 8×10^{-9} torr for 892 and 3453 hr, Respectively. Etchant: glyceria regia. 500x



Y-49010

613 hr

6.59×10^{-4} mg/cm²/hr



Y-50729

3453 hr

3.90×10^{-4} mg/cm²/hr

Fig. 13. As-Evaporated Surfaces of Type 316 Stainless Steel Tested at 872°C and 8×10^{-9} torr for 613 and 3453 hr, Respectively. Original magnification: 200X

in Fig. 12 that the 892-hr test resulted in surface ferrite while the 3453-hr test showed no indication of the presence of ferrite. Further, it is seen in Fig. 13 that the evaporated surface of the 3453-hr test contains annealing twins which are usually due to the face-centered cubic structure, but ferrite is a body-centered cubic structure. In addition, all short-term test specimens were magnetic while the long-term tests (> 1000 hr) were nonmagnetic, and ferrite could not be detected by x-ray analysis.

When the surfaces of short-term test specimens transformed to ferrite, the evaporation rate of type 316 stainless steel approached that for pure iron. For example, at 982°C the evaporation rate of pure iron was measured to be constant and equal to 6.2×10^{-3} mg/cm²/hr while the final rate for type 316 stainless steel was 6.64×10^{-3} mg/cm²/hr for a 650-hr test.

The experimental data have shown that the evaporation rates changed with time at a constant temperature. Therefore, the variation of evaporation rates with temperature was compared at approximately equal times. On this basis, Fig. 14 was drawn to provide a means of predicting the rates at temperatures below 750°C where accurate data were difficult to obtain.

Oxidized Surfaces

Several specimens oxidized in wet hydrogen were evaporated at 982, 927, 872, and 760°C . The Cr₂O₃ layer formed on the specimen surfaces retarded the evaporation of the base metal for varying periods of time, depending on the evaporation temperature. At the three higher temperatures, the Cr₂O₃ films deteriorated initially at the intersection of the surface with the grain boundaries, where evaporation of the more volatile elements and impurities occurred. This resulted in a semi-continuous network of voids. The remaining Cr₂O₃ film became progressively thinner due to evaporation and to a carbon-oxygen reaction which resulted in the formation of carbon monoxide. Subsurface voids attributed to the diffusion and condensation of lattice vacancies increase in size and number with increasing temperature. Simultaneous loss of austenite stabilizers resulted in the formation of surface ferrite at

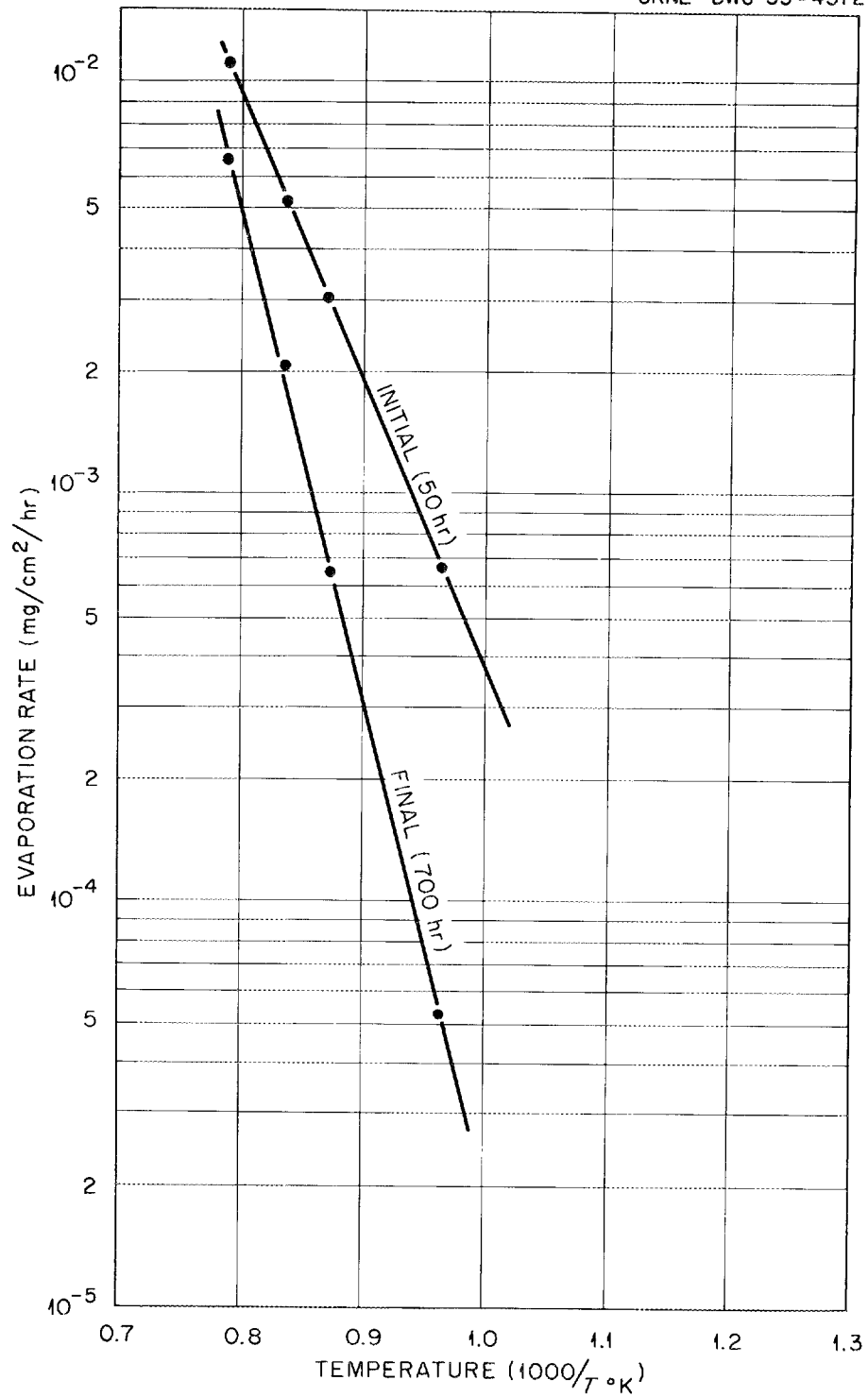
UNCLASSIFIED
ORNL-DWG 63-4372

Fig. 14. Variation with Temperature of Initial and Final Evaporation Rates for Type 316 Stainless Steel.

982 and 927°C for short-term tests, while at 872°C no ferrite was detected in a 1456-hr test. At 760°C, the Cr₂O₃ film was fully protective against evaporation losses of the base metal, at least to 1142 hr. These evaporation effects are metallographically illustrated in Fig. 15 while the results of the evaporation tests are summarized in Table 7 and presented graphically in Fig. 16. Comparison of the data in Table 7 with that previously presented in Table 5 indicates the degree of protection afforded by Cr₂O₃ films. When the Cr₂O₃ film is reduced by the carbon in the alloy at the alloy grain boundaries, evaporation of the alloy proceeds as illustrated in Fig. 17.

Table 7. Experimental Evaporation Rates of Type 316 Stainless Steel Preoxidized in Wet Hydrogen at 870°C

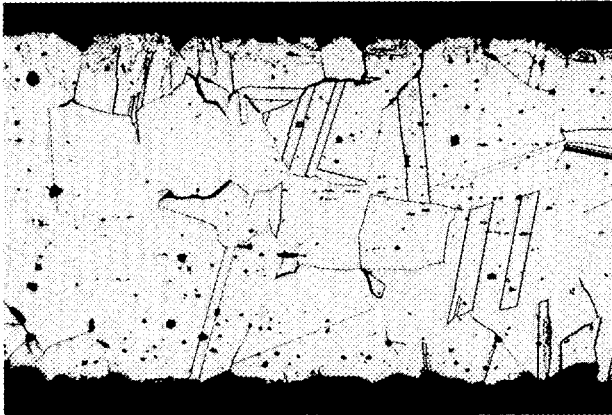
Evaporation Temperature (°C)	Duration of Test (hr)	Evaporation Rates (mg/cm ² /hr) × 10 ⁻⁴		Oxygen Pickup (mg/cm ²)	Final Oxide Layer
		Initial	Final		
982	1058	26.9	35.7	0.2804	Cr ₂ O ₃
927	1226	7.89	12.5	0.2983	Cr ₂ O ₃
872	1456	4.42	4.44	0.3134	Cr ₂ O ₃ + MnO ₂ (trace)
760	1142	No weight loss		0.2525	Cr ₂ O ₃

CONCLUSIONS

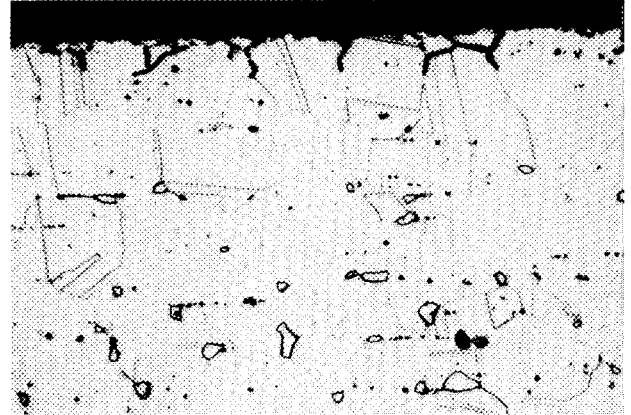
This study has shown that multicomponent iron-, nickel-, and cobalt-base alloys containing high vapor pressure elements such as chromium and manganese exhibit two modes of free evaporation from the solid state.

1. An initial high rate of surface evaporation due to the normal presence of the high vapor pressure elements.
2. Evaporation from the edges of surface grains, resulting in grain boundary grooving.

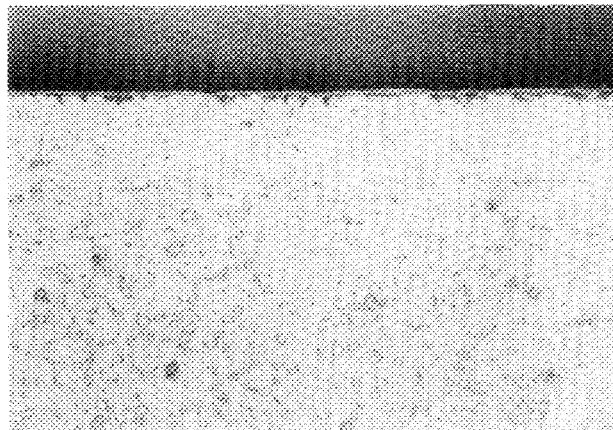
Once the surface became depleted of the higher vapor pressure elements, further loss of these elements was dependent on their diffusion rate in the base alloy. At the lower temperatures (< 900°C), the slow diffusion rates of the volatile, evaporating elements resulted in

UNCLASSIFIED
PHOTO-62802

982 °C
1058 hr
0.2804 mg/cm² O₂ PICKUP
ORIG. MAG. 500 X
Y-49179



872 °C
1456 hr
0.3134 mg/cm² O₂ PICKUP
ORIG. MAG. 1000 X
Y-50727



760 °C
1142 hr
0.2525 mg/cm² O₂ PICKUP
ORIG. MAG. 1500 X
Y-51219

Fig. 15. Type 316 Stainless Steel Oxidized in Wet Hydrogen and Subsequently Evaporation Tested in High Vacuum. Reduced 49%.

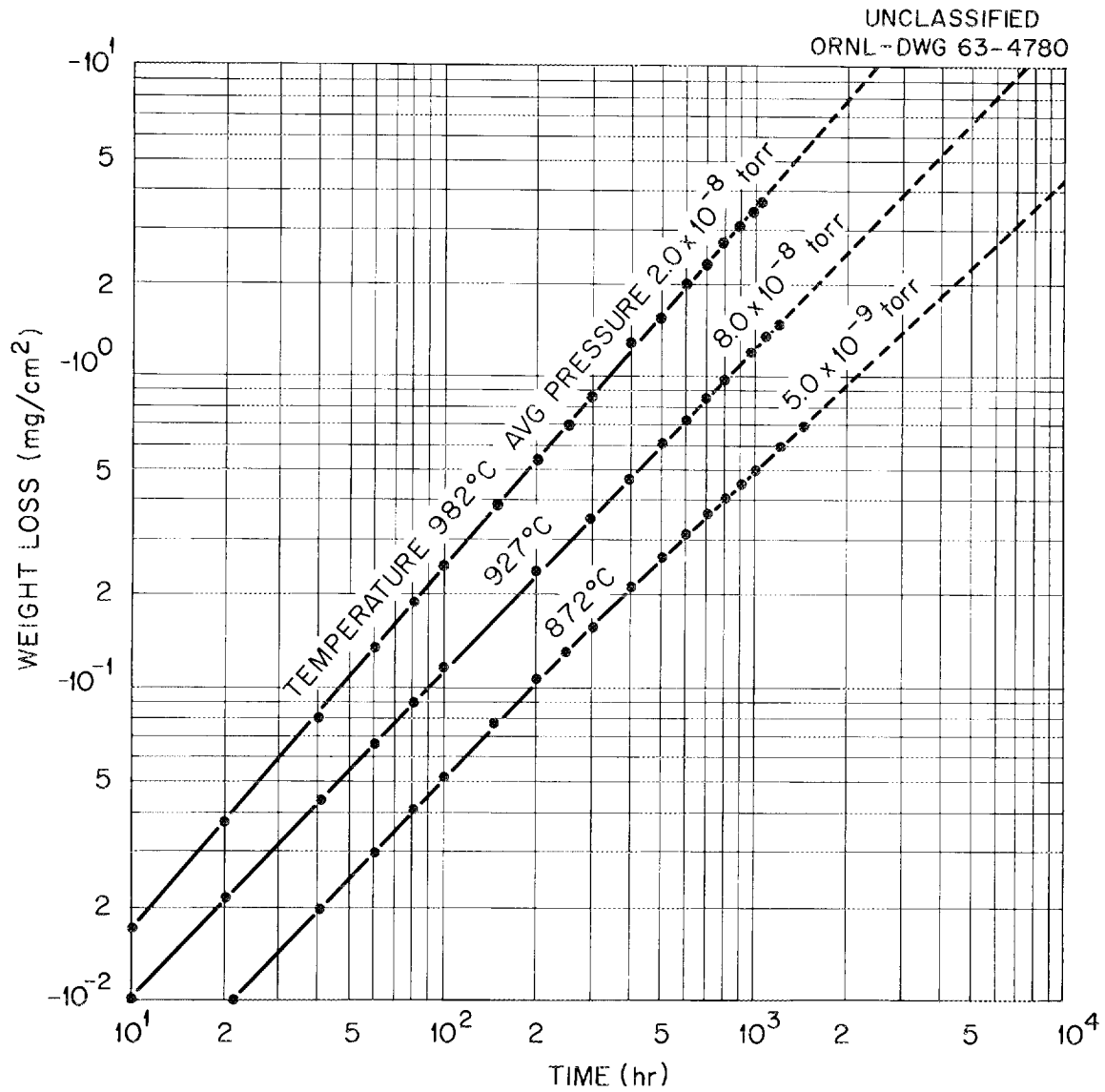


Fig. 16. Evaporation Losses of Type 316 Stainless Steel Oxidized in Wet Hydrogen at 825°C for 170 hr.

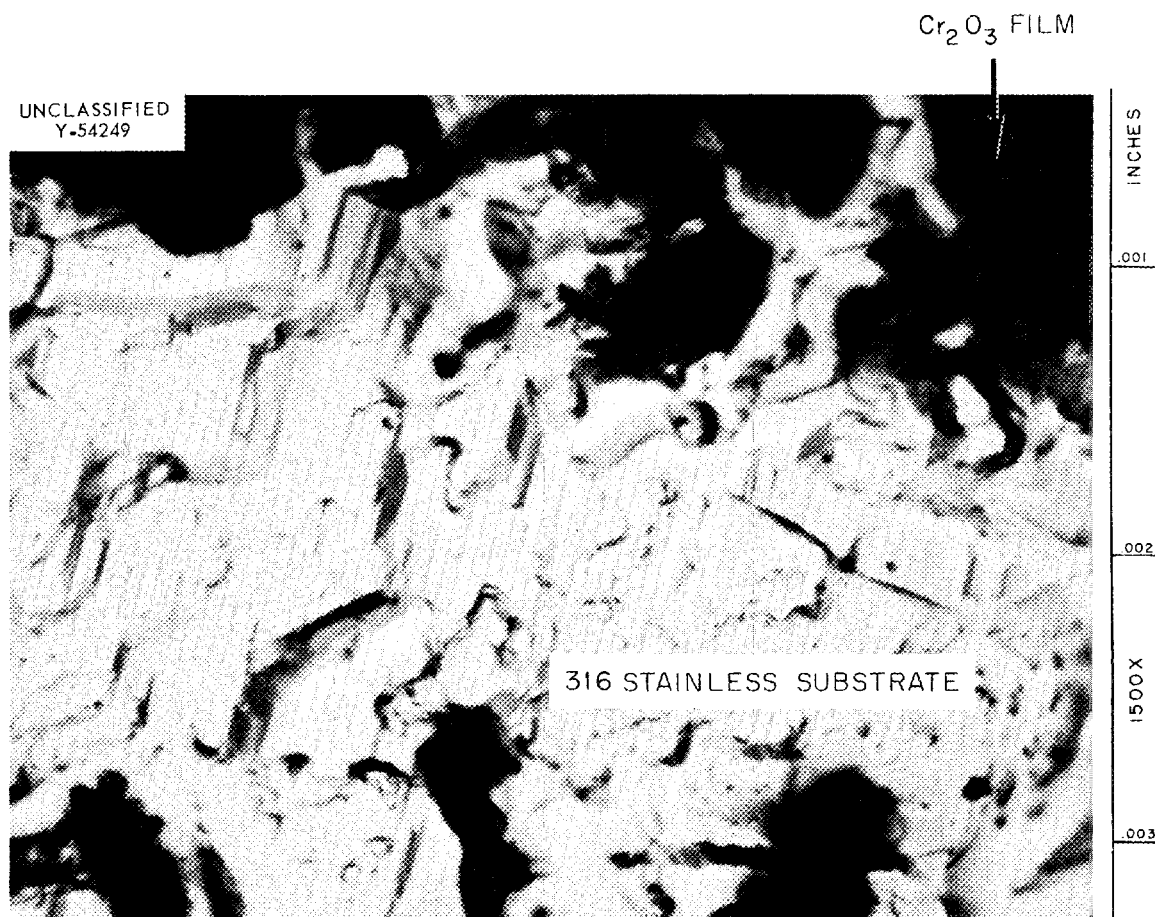


Fig. 17. As-Evaporated Surface of Type 316 Stainless Steel Oxidized in Wet Hydrogen and Subsequently Tested at 872°C and 2×10^{-8} torr for 2900 hr. 1500X

concentration gradients; however, at temperatures of 980°C or above, these concentration gradients were difficult to detect and the evaporation losses were more nearly constant with time. However, in either case a change in alloy composition occurred, and for type 316 stainless steel, the loss of austenite stabilizers resulted in ferrite precipitation at the specimen surfaces for short-term tests (< 1000 hr). In the case of Haynes alloy No. 25, the precipitates near the surfaces disappeared; however, grain boundary evaporation was not evident.

When the surfaces of the alloys investigated were oxidized in air, the initial evaporation rates decreased. However, after a transition period, the length of which was temperature dependent, the final rates were accelerated due to the deterioration of the oxide film at the surface-grain boundary intersection.

The evaporation of the oxides formed in air showed that Cr₂O₃ was the most stable. Type 316 stainless steel coated with Cr₂O₃ did not initially evaporate as rapidly as the polished surfaces; however, the final rates at 872, 927, and 982°C were great enough to rule out adequate protection against evaporation of the base alloy by this technique. At 760°C, however, Cr₂O₃ fully retarded evaporation of type 316 stainless steel, at least for 1150 hr, probably because carbon diffusion in the base alloy is sluggish (at this temperature) and most of the carbon is tied up as carbides.

Several considerations, therefore, make the theoretical prediction of the evaporation rates extremely difficult, if not impossible; these include compositional changes, phase transformation, areas of preferential evaporation, grain size, and decomposition of compounds.

ACKNOWLEDGMENTS

The author is indebted to the many service departments in carrying out various phases of these experiments. The assistance of R. M. Steele for the x-ray analysis, the analysis performed by W. R. Iaing of the Analytical Chemistry Division, and the metallographic work of W. R. Farmer proved to be necessary services in the interpretation of these experiments. The assistance of S. H. Wheeler and J. Newsome in carrying out the

experiments is appreciated. Discussions with G. P. Smith, J. V. Cathcart, and H. Inouye of the Metals and Ceramics Division were instrumental in the formulation of the conclusions reached in this investigation.

ORNL-3677
 UC-25 - Metals, Ceramics, and Materials
 TID-4500 (34th ed.)

INTERNAL DISTRIBUTION

- | | |
|-------------------------------------|----------------------------------|
| 1-3. Central Research Library | 77. T. S. Lundy |
| 4. Reactor Division Library | 78. H. G. MacPherson |
| 5-6. ORNL - Y-12 Technical Library | 79. H. E. McCoy, Jr. |
| Document Reference Section | 80. J. F. Murdock |
| 7-46. Laboratory Records Department | 81. M. L. Picklesimer |
| 47. Laboratory Records, ORNL R.C. | 82. G. Samuels |
| 48. ORNL Patent Office | 83. H. W. Savage |
| 49-53. D. T. Bourgette | 84. J. E. Savolainen |
| 54. J. Burka | 85. C. E. Sessions |
| 55. R. S. Crouse | 86. G. M. Slaughter |
| 56. F. L. Culler | 87. J. T. Stanley |
| 57. J. E. Cunningham | 88. R. M. Steele |
| 58. J. H. Frye, Jr. | 89. R. L. Stephenson |
| 59. R. G. Gilliland | 90. J. O. Stiegler |
| 60. T. G. Godfrey | 91. J. A. Swartout |
| 61. G. Hallerman | 92. A. Taboada |
| 62. J. P. Hammond | 93. J. W. Tackett |
| 63. R. L. Heestand | 94. W. C. Thurber |
| 64. D. M. Hewette II | 95. A. M. Weinberg |
| 65-69. M. R. Hill | 96. W. J. Werner |
| 70. D. O. Hobson | 97-116. G. D. Whitman |
| 71. H. W. Hoffman | 117. R. P. Wichner |
| 72. H. Inouye | 118. M. B. Bever (consultant) |
| 73. D. H. Jansen | 119. A. A. Burr (consultant) |
| 74. G. W. Keilholtz | 120. J. R. Johnson (consultant) |
| 75. C. E. Larson | 121. A. R. Kaufmann (consultant) |
| 76. C. F. Leitten, Jr. | |

EXTERNAL DISTRIBUTION

122. C. M. Adams, Jr., MIT
- 123-124. D. F. Cope, AEC, ORO
125. J. L. Gregg, Bard Hall, Cornell University
126. J. Simmons, AEC, Washington
127. E. E. Stansbury, University of Tennessee
128. D. K. Stevens, AEC, Washington
129. Research and Development Division, AEC, ORO
- 130-638. Given distribution as shown in TID-4500 (34th ed.) under Metals, Ceramics, and Materials category